

New Compact Design For Short Range Wireless Power Transmission at 1GHz Using H-Slot Resonators

Sherif Hekal¹, Adel B. Abdel-Rahman^{1,2}

¹ ECE department, Egypt-Japan University of Science and Technology, E-JUST, Alex, Egypt, sherif.hekal@ejust.edu.eg

² Faculty of Engineering, South Valley University, Qena, Egypt, adel_b15@yahoo.com

Abstract—In this paper, we present a new design for short range wireless power transfer using two compact size H-slot resonators. These quasi-lumped element resonators can transfer power through electromagnetic resonant coupling with high efficiency and compact structures. The proposed design enables us to achieve power transfer efficiency of 85% at distance 5 mm. The new proposed design has been fabricated and measured to operate at 1 GHz. Measurements have shown consistency with simulation results and theoretical studies.

Index Terms—Defected ground structures, coupled resonators, quasi-lumped elements, wireless power transfer.

I. INTRODUCTION

The technology of wireless power transfer (WPT) has attracted a great attention in the last decades for its wide potential applications like RFIDs [1], portable electronic devices (mobile phones, tablets, etc.) [2], [3], wireless sensors [4], [5], and implantable biomedical devices [6], [7]. For long term, this will make our lives easy and hassle free. There will be no need for non-rechargeable batteries, wires and cords at small or large scale.

The methods of implementation can be categorized into three main classes: 1) Electromagnetic induction that can be found in the form of magnetic coupling [8], [9] and capacitive coupling [10], [11]. This method is preferred for short range WPT. 2) Electromagnetic resonant coupling using the resonance of transmitter and receiver circuits to focus power at a certain frequency to achieve high efficiency. This technique can be found in mid-range applications [12]. 3) Electromagnetic transmission is used for long range power transmission over few thousands of meters by using microwave transmissions or laser beams [13], [14].

Almost all the mentioned techniques in electromagnetic induction or resonant coupling have been depended upon lumped elements like inductors and capacitors, which have some disadvantages: bulky, occupy large area, and high losses; however, they are preferred in low frequency applications. Other designs have used printed spirals with series or shunt surface mounted capacitors to get compact WPT systems that are suitable for board-to-board applications and biomedical implants, as reported in [15]–[18], but somehow experience low efficiency. In [19], [20], the authors have verified that the optimal operating frequency for biological media is at the GHz-

range for high power gain and structure miniaturization. We intend here to use defected ground structures (DGSs) that behave like quasi-lumped LC resonant circuits [21]–[23]. These compact structures have good advantages such as small sizes, little volume, low losses, and low cost. A comparative study between different shapes of DGSs, acting as band rejection at the same resonance frequency, has been reported in [24]. The study has proved that the H-slot DGS, rather than other shapes, has the smallest size and the highest quality factor.

In this paper, we present a new compact design that can be applied to short range WPT systems like board-to-board applications, biomedical implants, and electronic portable devices. A detailed analysis of a compact H-slot DGS as parallel LC resonator is discussed. Comparison between H-slot resonator and its equivalent circuit is performed using electromagnetic simulator (CST microwave studio) and RF circuit simulator (ADS) respectively. An analytic model is developed for two coupled H-slot resonators with investigation of the coupling performance. For verification, the new proposed WPT system has been fabricated and measured.

II. DESIGN MODEL & SIMULATION

A. Single H-slot resonator

The implementation of quasi-lumped elements based on DGSs has been discussed in [21]–[23]. These structures have been proposed for RF/Microwave applications to implement band-pass and band-stop filters with low profiles. As illustrated in Fig. 1(a), the solid line between port (P_1) and port (P_2) represents the 50Ω feed line at the top layer of substrate while the dashed line represents the H-slot defected in ground plane. Fig. 1(b) represents the circuit model of single H-slot resonator.

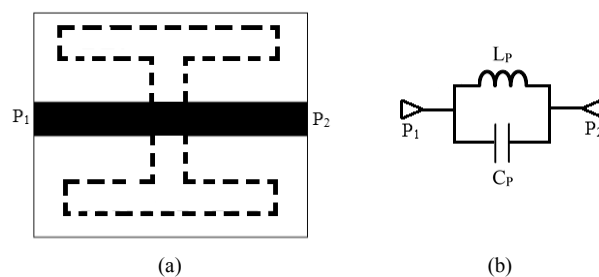


Fig. 1. (a) H-slot resonator. (b) Circuit model of H-slot resonator.

This design is implemented on EM simulator as shown in Fig. 2, using the detailed design parameters in Table I, to get response of one pole band-stop filter ($f_0 = 1.29$ GHz and $f_c = 0.94$ GHz) where f_0 is the pole frequency and f_c is the lower cutoff frequency at -3dB. This design will be modified later in the section of coupled resonators to be suitable for operating frequency of 1GHz.

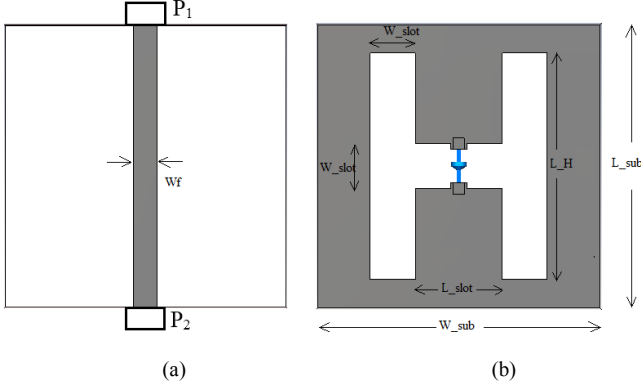


Fig. 2. Implementation of H-slot resonator on CST (a) top layer. (b) bottom layer

TABLE I. DESIGN PARAMETERS OF H-SLOT RESONATOR

parameter	value	parameter	value
L_{sub}	25 mm	L_H	20 mm
W_{sub}	25 mm	Substrate	Rogers 4003 ($\epsilon_r = 3.38$)
W_f	2.1 mm	thickness	0.813mm
W_{slot}	4 mm	Metal thickness	35 μ m
L_{slot}	7.5 mm	SMD Cap	1pF

A surface mounted capacitor of 1 pF is added to the slot to increase its equivalent capacitance without increasing the dimensions of structure leading to a compact resonator with high quality factor [25]. In order to verify the agreement between H-slot resonator and its circuit model in Fig. 1(b), we need first to extract the equivalent circuit parameters (L_P and C_P) from the EM simulation results. Following the work in [21], [22] and its detailed explanation in [26], we can extract the values of L_P and C_P using the equations of frequency and element transformation from low pass prototype to one pole Butterworth band-stop filter as follows

$$C_P = \frac{5f_c}{\pi[f_0^2 - f_c^2]} \quad \text{pF} \quad (1)$$

$$L_P = \frac{250}{C_P[\pi f_0]^2} \quad \text{nH} \quad (2)$$

By substituting with the values of $f_0 = 1.29$ GHz and $f_c = 0.94$ GHz in (1) and (2), we get $L_P = 8$ nH and $C_P = 1.9$ pF. The circuit model with calculated values of L_P and C_P will be simulated. As Shown in Fig. 3, we can perceive good agreement between the resonator and its circuit model. The proposed resonator can be considered as a building block for two coupled resonators that can transfer power.

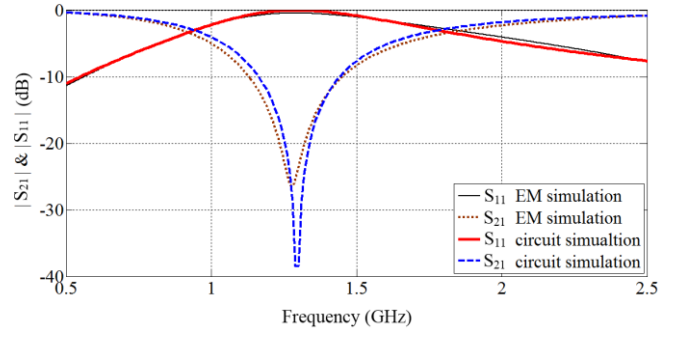


Fig. 3. S parameters of H-slot resonator and its circuit model

B. Two coupled H-slot resonators

In the previous section, we presented an analytic design method for parallel LC resonant circuit using a compact H-slot DGS. In this section, we study the behavior of two coupled H-slot resonators. First, the single H-slot resonator is modified as shown in Fig. 4 with the same dimensions mentioned in Table I, where a stub of length S is added to the feed line with length L_f . The stub behaves like a series capacitor C_S , which is used for adjusting the resonant frequency and impedance matching by tuning its length.

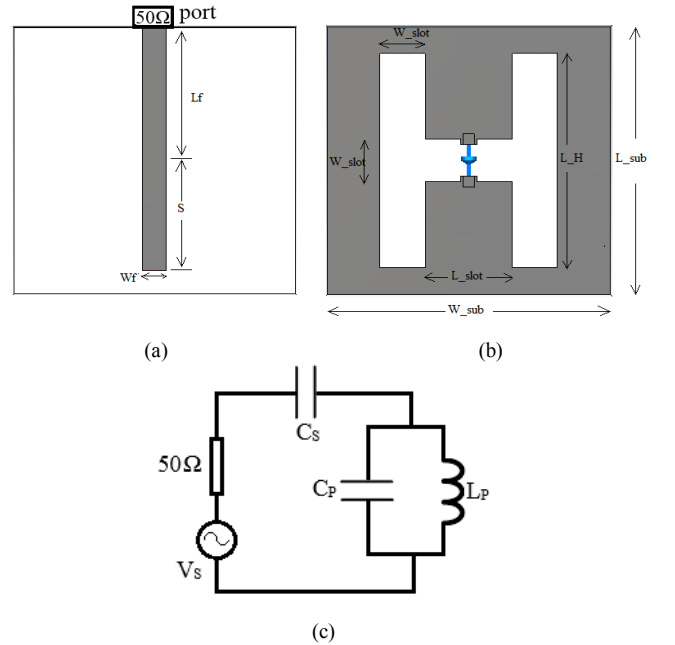
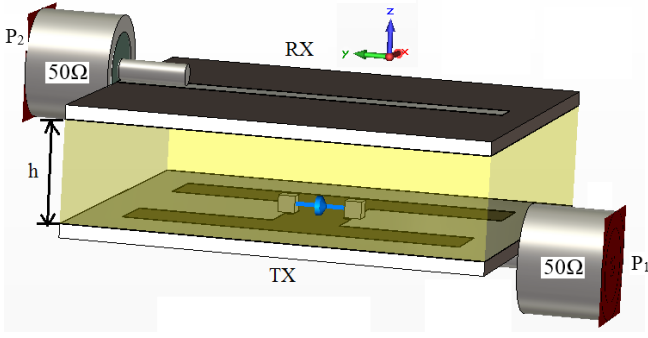
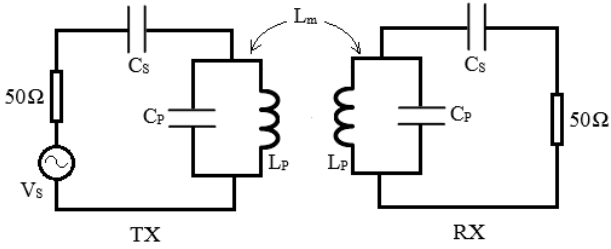


Fig. 4. H-slot resonator with adding stub. (a) top layer. (b) bottom layer (c) circuit model of modified H-slot resonator

Fig. 5(a) shows the proposed design of two coupled H-slot resonators which are separated by distance h (mm). Fig. 5(b) shows the circuit model of the proposed design. The system of the two coupled resonators shown in Fig. 5(a) is implemented and simulated using EM simulator with the same design parameters in Table I. The stub length $S = 11$ mm and the medium between the coupled resonators is foam with $\epsilon_r = 1.2$.

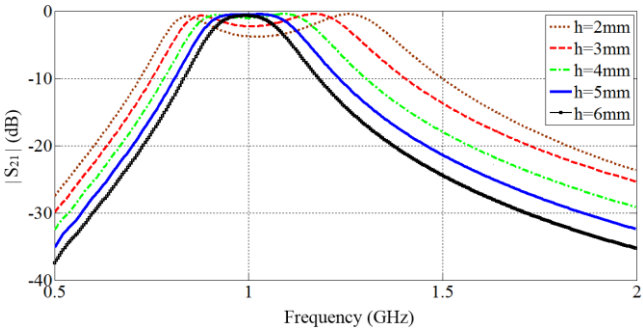


(a)

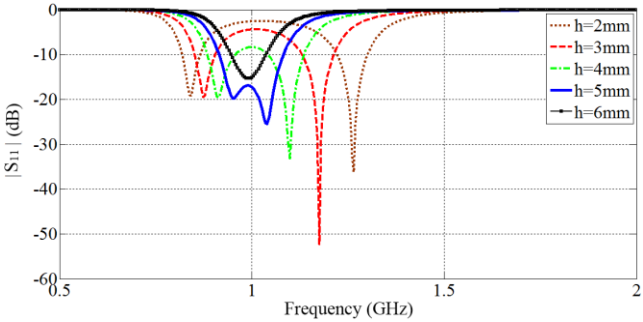


(b)

Fig. 5. Proposed H-slot coupled resonators (a) implementation on EM simulator (b) Circuit model of the two coupled resonators



(a)



(b)

Fig. 6. S parameters of the two H-slot coupled resonators with variable in-between distance h (a) S_{21} . (b) S_{11}

By changing the distance between the two resonators, we notice the change of coupling coefficient K from high values at short distances (mutual coupling is strong) to low values at long distances (mutual coupling is weak). At short distances, the coupling is strong enough to make each resonator affects the

other one and splitting of resonant frequency is occurred such that two peaks appear around the central frequency f_s . These two peaks are called electric and magnetic walls f_e and f_m . This phenomenon of splitting has been studied in detail in [27] and the coupling coefficient can be defined as

$$K = \frac{L_m}{L_P} = \frac{f_e^2 - f_m^2}{f_e^2 + f_m^2} \quad (3)$$

Where K is the coupling coefficient, L_P is the self-inductance, and L_m is the mutual inductance between inductors.

Fig. 6 explains how the change in distance h affects the coupling coefficient K and so the power that can be transferred from transmitter to receiver. As illustrated in Fig. 6, a maximum power transfer with insertion loss $S_{21} = -0.54$ dB is achieved at central frequency $f_s = 1$ GHz and a separation distance $h = 5$ mm.

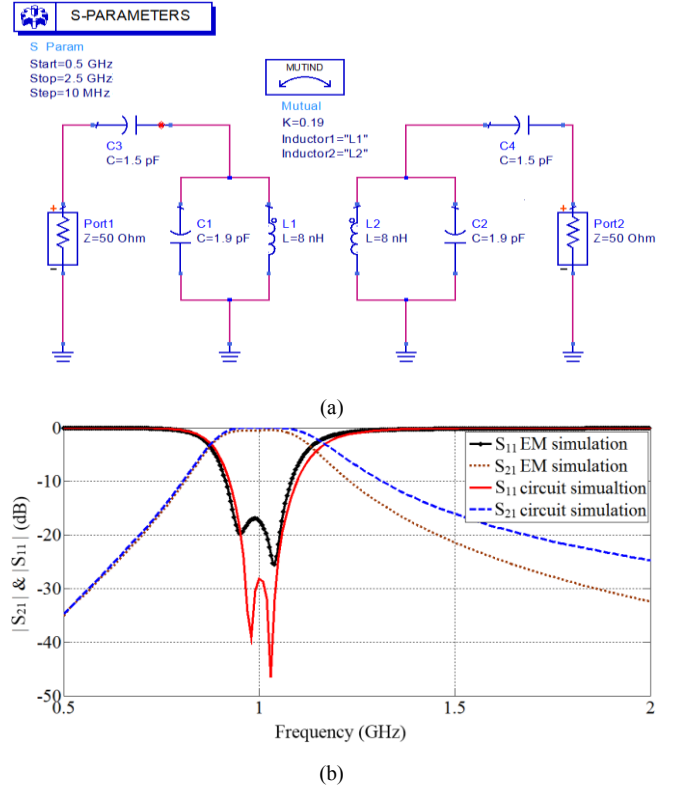


Fig. 7. Circuit model of the two H-slot coupled resonators (a) Implementation on circuit simulator. (b) Comparison between circuit and EM simulation results of the S parameters

At any frequency $f < f_0$, the parallel resonant circuit $L_P C_P$ behaves as inductor L_{eq} where

$$L_{eq} = \frac{L_P}{[1 - (\frac{f}{f_0})^2]} \quad \text{nH} \quad (4)$$

So, the equivalent circuit of each resonator will be L_{eq} in series with C_S . the value of C_S can easily be calculated from

$$C_S = \frac{1}{4\pi^2 f_s^2 L_{eq}} \quad \text{pF} \quad (5)$$

By substituting with values of $f_0 = 1.29$ GHz, $f_c = 0.94$ GHz, and $f_s = 1$ GHz in (4)-(5) we get $C_S = 1.5$ pF. The circuit model is

implemented as shown in Fig. 7(a). As illustrated in Fig. 7(b), good agreement between the results of EM and circuit simulations.

III. MISALIGNMENT STUDY

One of the most critical factors that affect the efficiency of WPT systems is the misalignment between TX and RX. Misalignment has been investigated by fixing the TX resonator and shift the RX resonator for the proposed structure, shown in Fig. 5(a). It can be inferred from the EM simulation results in Table II that normal decay occurred in the efficiency as the RX is shifted away from the TX in X and Y directions. A remarkable decay occurred in X shift especially at shift of 6 mm, that is equal to half of $(L_{\text{slot}} + W_{\text{slot}})$, where position of maximum magnetic field of TX faces position of minimum magnetic field of RX and so no coupling happened.

TABLE II. MISALIGNMENT INVESTIGATION

Shift (mm)	Power Transfer Efficiency (%)	
	shift in X direction	shift in Y direction
0	89	89
2	89	88
4	59	88
6	0	86
8	46	82
10	79	74
12	82	62
14	75	45
16	52	28
18	22	14
20	5	5
22	0	1
24	0	1

IV. FABRICATION AND MEASUREMENTS

The new proposed design for short range WPT was fabricated with the same design parameters in Table I, distance between the two resonators $h = 5$ mm, and material in between is foam as shown in Fig. 8(a). Fig. 8(b) shows the measurement setup for the fabricated WPT system using a network analyzer (Agilent N5227A) after making full two-port calibration. Fig. 8(c) shows the simulated and measured responses of the proposed WPT system. It is noticed that good agreement between predicted EM simulation and carried out measurements. The measured response has $S_{21} = -0.73$ dB and $S_{11} = -23$ dB at a central frequency of 1GHz with bandwidth of 200MHz. Wide bandwidth is a good advantage to ingest the output frequency deviations from non-perfect commercial oscillators. The efficiency of power transfer is defined as the ratio of output power at port2 (RX) to the input power at port1 (TX). Fig. 9 shows the measured and simulated efficiency of the new WPT system at different separations h . It is easily noticed that maximum measured efficiency of 85% can be achieved at distance $h = 5$ mm.

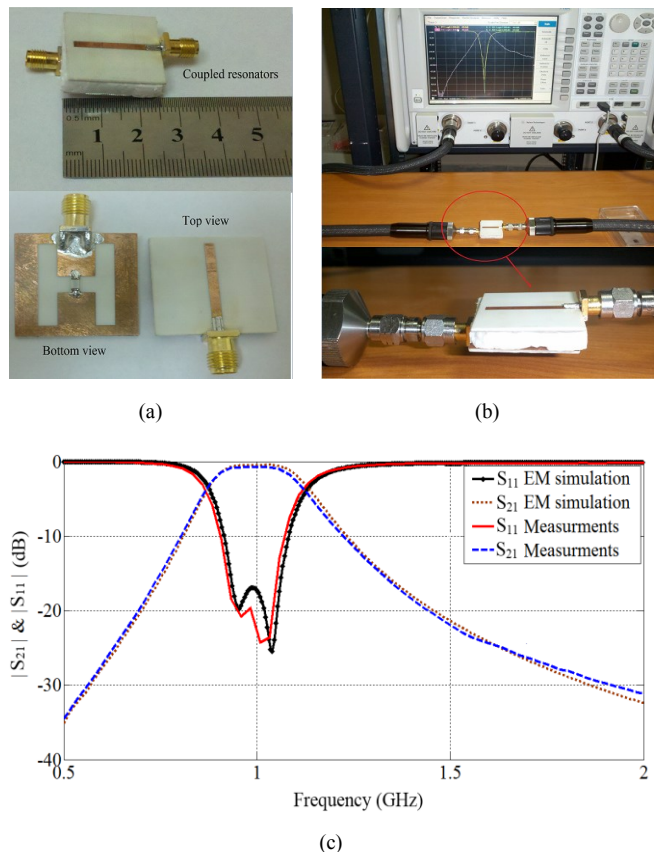


Fig. 8. Fabrication and experimental measurements of the WPT system (a) Fabrication. (b) Measurements setup using network analyzer. (c) Simulated and measured S parameters

The power handling capability is limited by heating caused by conductor and dielectric losses. The used substrate RO4003, with thermal conductivity of 0.65 and loss tangent of 0.0027, has been tested over free software MWI to calculate the temperature rise per RF power and was found 0.18 C°/W. our proposed structure can be used for low or medium power applications. Modifications for the structure like increasing metal thickness can be made in order to be suitable for high power applications.

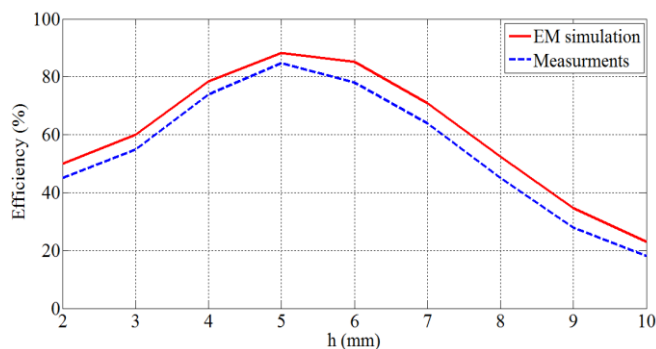


Fig. 9. Simulated and measured Efficiency for the new WPT system vs. the distance h .

V. CONCLUSION

In this paper, a novel structure for short range WPT has been presented. This structure is composed of two compact size H-slot resonators that can transfer power, with a good efficiency of 85% at short distance 5 mm, using electromagnetic resonant coupling. This structure is suitable for small size appliances like board-to-board applications, biomedical implants, and charging personal portable devices. Analytic models for single and coupled resonators were developed and implemented on EM and circuit simulator to verify the design theory. Good agreement between predicted and measured results has been achieved.

VI. ACKNOWLEDGMENT

We would like to acknowledge the Electronics Research Institute (ERI) - Microstrip Department, for the support, encouragement, help and cooperation during the simulation process of this research. This work was supported by the Ministry of Higher Education (MoHE), Egypt and the Egypt-Japan University of Science and Technology (E-JUST).

REFERENCES

- [1] M. Kiani and M. Ghovanloo, "An RFID-Based Closed-Loop Wireless Power Transmission System for Biomedical Applications," *IEEE Trans. Circuits Syst. II Express Briefs*, vol. 57, no. 4, pp. 260–264, Apr. 2010.
- [2] S. Kim, I. Cho, J. Moon, S. Jeon, and J. Choi, "5W wireless power transmission system with coupled magnetic resonance," in *IEEE 5th International Symposium on Microwave, Antenna, Propagation and EMC Technologies for Wireless Communications (MAPE)*, Chengdu, 2013, pp. 255–258.
- [3] Z. Yalong, H. Xueliang, Z. Jiaming, and T. Linlin, "Design of wireless power supply system for the portable mobile device," in *IEEE International Wireless Symposium (IWS)*, Beijing, 2013, pp. 1–4.
- [4] O. Jonah and S. V. Georgakopoulos, "Wireless power transmission to sensors embedded in concrete via magnetic resonance," in *IEEE 12th Annual Wireless and Microwave Technology Conference (WAMICON)*, Clearwater Beach, FL, 2011, pp. 1–6.
- [5] O. Jonah and S. V. Georgakopoulos, "Wireless Power Transfer in Concrete via Strongly Coupled Magnetic Resonance," *IEEE Trans. Antennas Propag.*, vol. 61, no. 3, pp. 1378–1384, Mar. 2013.
- [6] B. M. Badr, R. Somogyi-Gsizmazia, N. Dechev, and K. R. Delaney, "Power transfer via magnetic resonant coupling for implantable mice telemetry device," in *IEEE Wireless Power Transfer Conference (WPTC)*, Jeju, 2014, pp. 259–264.
- [7] M. Zargham and P. G. Gulak, "A 0.13 μm CMOS integrated wireless power receiver for biomedical applications," in *Proceedings of the ESSCIRC (ESSCIRC)*, 2013, pp. 137–140.
- [8] T. J. Parks and D. S. Register, "Inductive coupling system for power and data transfer," *US5455466 A*, 03-Oct-1995.
- [9] S. K. Yoon, S. J. Kim, and U.-K. Kwon, "A new circuit structure for near field wireless power transmission," in *IEEE International Symposium on Circuits and Systems (ISCAS)*, Seoul, 2012, pp. 982–985.
- [10] A. Rozin and G. Kaplun, "Capacitively coupled bi-directional data and power transmission system," *US5847447 A*, 08-Dec-1998.
- [11] M. E. Karagozler, J. D. Campbell, G. K. Fedder, S. C. Goldstein, M. P. Weller, and B. W. Yoon, "Electrostatic latching for inter-module adhesion, power transfer, and communication in modular robots," in *IEEE/RSJ International Conference on Intelligent Robots and Systems*, San Diego, CA, IROS 2007, pp. 2779–2786.
- [12] A. Kurs, A. Karalis, R. Moffatt, J. D. Joannopoulos, P. Fisher, and M. Soljačić, "Wireless Power Transfer via Strongly Coupled Magnetic Resonances," *Science*, vol. 317, no. 5834, pp. 83–86, Jul. 2007.
- [13] H. Matsumoto, "Research on solar power satellites and microwave power transmission in Japan," *IEEE Microw. Mag.*, vol. 3, no. 4, pp. 36–45, 2002.
- [14] J. O. McSpadden and J. C. Mankins, "Space solar power programs and microwave wireless power transmission technology," *IEEE Microw. Mag.*, vol. 3, no. 4, pp. 46–57, 2002.
- [15] S. Kong, et al., "Analytical expressions for maximum transferred power in wireless power transfer systems," in *IEEE International Symposium on Electromagnetic Compatibility (EMC)*, Long Beach, CA, Aug. 2011, pp. 379–383.
- [16] S. Kim, et al., "Design, implementation and measurement of board-to-board wireless power transfer (WPT) for low voltage applications," in *22nd IEEE Conference on Electrical Performance of Electronic Packaging and Systems (EPEPS)*, San Jose, CA, Oct. 2013, pp. 91–95.
- [17] S. Kim, et al., "Electromagnetic interference shielding effects in wireless power transfer using magnetic resonance coupling for board-to-board level interconnection," in *IEEE International Symposium on Electromagnetic Compatibility (EMC)*, Denver, CO, Aug. 2013, pp. 773–778.
- [18] M. Falavarjani, M. Shahabadi, and J. Rashed-Mohassel, "Design and implementation of compact WPT system using printed spiral resonators," *IET Electron. Lett.*, vol. 50, no. 2, pp. 110–111, Jan. 2014.
- [19] A. S. Poon, S. O'Driscoll, and T. H. Meng, "Optimal operating frequency in wireless power transmission for implantable devices," in *IEEE 29th Annual International Conference in Engineering in Medicine and Biology Society (EMBS)*, Lyon, Aug. 2007, pp. 5673-5678.
- [20] A. S. Poon, S. O'Driscoll, and T. H. Meng, "Optimal frequency for wireless power transmission into dispersive tissue," *IEEE Trans. Antennas Propag.*, vol. 58, no. 5, pp. 1739-1750, May 2010.
- [21] D. Ahn, et al., "A design of the low-pass filter using the novel microstrip defected ground structure," *IEEE Trans. Microw. Theory Tech.*, vol. 49, no. 1, pp. 86–93, Jan. 2001.
- [22] A. B. Abdel-Rahman, A. Verma, A. Boutejdar, and A. Omar, "Compact stub type microstrip bandpass filter using defected ground plane," *IEEE Microw. Wirel. Compon. Lett.*, vol. 14, no. 4, pp. 136–138, Apr. 2004.
- [23] S. U. Rehman, A. Sheta, and M. Alkanhal, "Compact bandstop filter using defected ground structure (DGS)," in *Saudi International Electronics, Communications and Photonics Conference (SIECPC)*, Riyadh, April 2011, pp. 1–4.
- [24] M. K. Mandal and S. Sanyal, "A novel defected ground structure for planar circuits," *IEEE Microw. Wireless Compon. Lett.*, vol. 16, no. 2, pp. 93-95, Feb. 2006.
- [25] A. B. Abdel-Rahman, and A. S. Omar, "Miniaturized bandpass filters using capacitor loaded folded slot coupled resonators," in *IEEE Middle East Conference on Antennas and Propagation (MECAP)*, Oct. 2010, pp. 1-4.
- [26] J.-S. Hong and M. J. Lancaster, *Microstrip Filters for RF/Microwave Applications*. John Wiley & Sons, 2004.
- [27] Y. Zhang, Z. Zhao, and K. Chen, "Frequency splitting analysis of magnetically-coupled resonant wireless power transfer," in *IEEE Energy Conversion Congress and Exposition (ECCE)*, Denver, CO, Sept. 2013, pp. 2227–2232.